



# Nutrient utilization and diatom productivity changes in the low-latitude south-eastern Atlantic over the past 70 ka: response to Southern Ocean leakage

Katharine Hendry<sup>1</sup>, Oscar Romero<sup>2,3</sup>, and Vanessa Pashley<sup>4</sup>

<sup>1</sup>University of Bristol, School of Earth Sciences, Bristol BS8 1RJ, UK

<sup>2</sup>MARUM – Center for Marine Environmental Sciences, University of Bremen, 28359 Bremen, Germany

<sup>3</sup>Alfred Wegener Institute, Helmholtz Centre for Polar and Marine Research, 27568 Bremerhaven, Germany

<sup>4</sup>Geochronology and Tracers Facility, British Geological Survey, Keyworth NG12 5GG, UK

**Correspondence:** Katharine Hendry (k.hendry@bristol.ac.uk)

Received: 31 August 2020 – Discussion started: 29 September 2020

Revised: 25 January 2021 – Accepted: 1 February 2021 – Published: 9 March 2021

**Abstract.** Eastern boundary upwellings (EBUs) are some of the key loci of biogenic silica (opal) burial in the modern ocean, representing important productive coastal systems that extraordinarily contribute to marine organic carbon fixation. The Benguela upwelling system (BUS), in the low-latitude south-eastern Atlantic, is one of the major EBUs and is under the direct influence of nutrient-rich Southern Ocean waters. Quantification of past changes in diatom productivity through time, in response to late Quaternary climatic change, feeds into our understanding of the sensitivity of EBUs to future climatic perturbations. Existing sediment archives of silica cycling include opal burial fluxes, diatom assemblages, and opaline silicon isotopic variations (denoted by  $\delta^{30}\text{Si}$ ). Burial fluxes and siliceous assemblages are limited to recording the remains reaching the sediment (i.e. export), and  $\delta^{30}\text{Si}$  variations are complicated by species-specific influences and seasonality. Here, we present the first combined  $\delta^{30}\text{Si}$  record of two large centric diatoms from the BUS, encompassing full glacial conditions to the Holocene. In addition to export, our new data allow us to reconstruct the utilization of dissolved Si in surface waters in an area with strong input from Southern Ocean waters. Our new archives show that there was enhanced upwelling of Southern Ocean Si-rich water accompanied by strong silicic acid utilization by coastal dwelling diatoms during Marine Isotope Stage 3 (MIS3; 60–40 ka). This pulse of strong silicic acid utilization was followed by a weakening of upwelling and coastal diatom Si utilization into MIS2, before an increase in pelagic diatom Si

utilization across the deglaciation. We combine our findings with mass balance model experiments to show that changes in surface water silica cycling through time are a function of both upwelling intensity and utilization changes, illustrating the sensitivity of EBUs to climatic change on glacial–interglacial scales.

## 1 Introduction

Marine productivity by diatoms represents up to half of the total fixation of organic matter in the oceans and plays a key role in uptake of carbon dioxide ( $\text{CO}_2$ ) from the atmosphere (Tréguer et al., 2018). Large-scale oceanic circulation is a first-order control on the present-day supply of dissolved silicon (silicic acid or DSi) to surface waters that is essential for diatom growth. In the modern ocean, the burial of biogenic silica (opal) is localized in regions characterized by a supply of DSi-rich waters: the Southern Ocean (SO), the subarctic Pacific, and in the eastern boundary upwellings (EBUs; Ragueneau et al., 2000). The Benguela upwelling system (BUS; Fig. 1) in the south-eastern (SE) Atlantic is one of the major EBUs and is under the influence of DSi-rich SO waters (Berger and Wefer, 1996; Berger et al., 2002). Quantification of BUS Si production in the late Quaternary is important for understanding the functioning of this highly productive EBU as well as the sensitivity of the strong and dynamic biological production to changes in wind-driven mixing and SO leakage and ventilation (Hendry and Brzezinski, 2014).

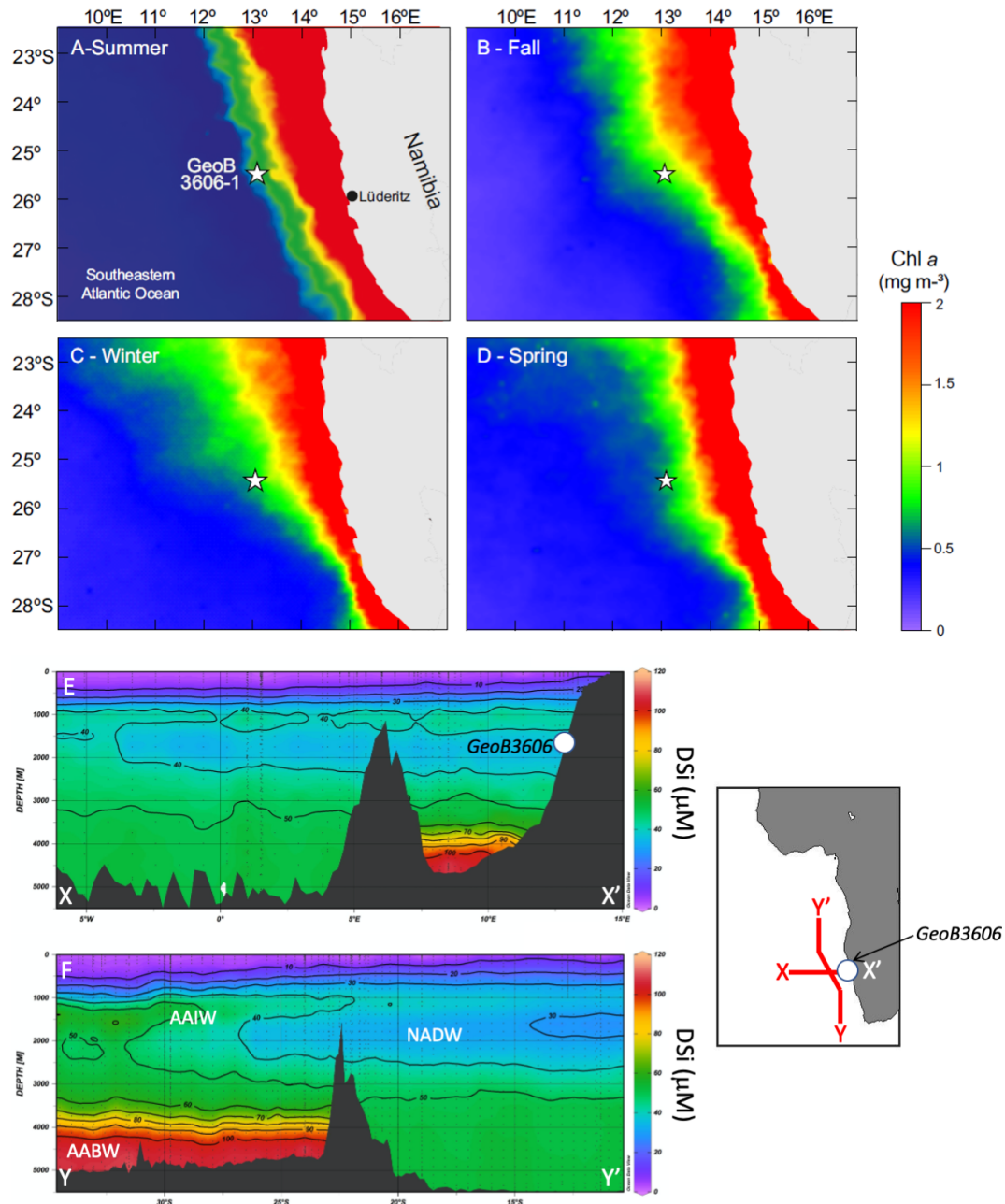


**Figure 1.** Location of the study site GeoB3606-1 (white star) in the Benguela upwelling system. Seasonally averaged concentration of chlorophyll *a* ( $\text{mg m}^{-3}$ ) for (a) January–March (austral summer), (b) April–June (austral fall), (c) July–September (austral winter), and (d) October–December (austral spring) from the years 1998 to 2009 at a  $9 \text{ km} \times 9 \text{ km}$  resolution (Goddard Space Flight Center, <http://oceancolor.gsfc.nasa.gov/SeaWiFS>, last access: 3 February 2020). (e–f) Sections showing DSi near the core location site in the modern Atlantic: (a) west–east transect (X–X′); (b) south–north transect (Y–Y′). The transects are shown using red lines in the insert; the approximate core location is shown using a circle.

The silicic acid leakage hypothesis (SALH) postulates that shifts in the leakage (i.e. export) of DSi, relative to other nutrients, within Antarctic Intermediate Water (AAIW; Fig. 1) could occur on glacial–interglacial timescales as a result of changes in SO diatom physiology and silicification due to the alleviation of iron stress from dust supply (Brzezinski

et al., 2002). The northward supply of waters with a higher DSi-to-nitrate ratio via AAIW during full glacials would promote low-latitude diatom growth at the expense of other non-siliceous phytoplankton. This assemblage shift would result in a weakening of the carbonate pump and a change in seawater alkalinity that would contribute to atmospheric car-

bon dioxide concentration ( $p\text{CO}_2$ ) drawdown (Matsumoto and Sarmiento, 2008). Opal burial and geochemical archives show that DSi leakage during the last glacial maximum (LGM) is variable, with some evidence for this mechanism in the South Pacific (Chase et al., 2003; Rousseau et al., 2016) but a patchy opal burial response in the equatorial Pacific (Kienast et al., 2006). In the Atlantic, there is stronger evidence that DSi leakage and opal production was higher during the deglacial rather than during the LGM (Hendry et al., 2016; Meckler et al., 2013). The impact of DSi leakage on opal burial during the deglacial is heterogeneous, both in the Atlantic and Pacific (Bradtmiller et al., 2006, 2007; Dubois et al., 2010), suggesting that the ventilation of DSi-rich waters is required to promote diatom growth (Hendry and Brzezinski, 2014). However, to date, there are no published archives of silicon cycling under full glacial conditions south of the subantarctic front. Furthermore, very few archives have been published over this time period from lower latitudes, although one record highlights potential SO leakage and increase in AAIW DSi in Marine Isotope Stage (MIS) 3–4 in the tropical north-western (NW) Atlantic (Griffiths et al., 2013). Analogous to carbon cycling, siliceous production can be considered as two interconnected processes: net utilization is the proportion of DSi taken up by diatoms to form opal in ocean surface waters, and export production is the opal that sinks out of the surface waters into the deep (Ragueneau et al., 2000). However, when reconstructing marine siliceous primary production, the only evidence available is the opal buried as siliceous remains of microorganisms within marine sediments. Understanding the link between surface DSi utilization, recycling, and export of opal is important to understand ecosystem function and organic matter sequestration. The stable Si isotopic composition (denoted in per mil relative to standard NBS28/RM8546 by  $\delta^{29}\text{Si}$  or more commonly  $\delta^{30}\text{Si}$ ; Eqs. 1, 2) of opal provides an archive of DSi utilization, given the preferential uptake of lighter Si isotopes during diatom biomineralization (De La Rocha et al., 1997).

$$\delta^{29}\text{Si}(\text{‰}) = \left( \frac{\left( \frac{^{29}\text{Si}}{^{28}\text{Si}} \right)_{\text{Sample}}}{\left( \frac{^{29}\text{Si}}{^{28}\text{Si}} \right)_{\text{NBS28}}} - 1 \right) \times 1000 \quad (1)$$

$$\delta^{30}\text{Si}(\text{‰}) = \left( \frac{\left( \frac{^{30}\text{Si}}{^{28}\text{Si}} \right)_{\text{Sample}}}{\left( \frac{^{30}\text{Si}}{^{28}\text{Si}} \right)_{\text{NBS28}}} - 1 \right) \times 1000 \quad (2)$$

Culture studies and field observations indicate that diatoms discriminate Si isotopes by a fractionation factor,  $\epsilon$ , of approximately  $-1.1\text{‰}$ , although estimates for this value range from  $-0.4\text{‰}$  to  $-2.5\text{‰}$  (Hendry and Brzezinski, 2014, and references therein). The application of this utilization proxy is complicated by several unknowns: changes in the initial isotopic composition of ambient seawater through time (Horn et al., 2011), potential seasonal and ecological bias

(Swann et al., 2017), and potential species-specific fractionation of Si isotopes in mixed assemblages (Sutton et al., 2013). Here, we present the first late Quaternary  $\delta^{30}\text{Si}$  records from the BUS during the full glacial conditions of Marine Isotope Stage (MIS) 4 to the late Holocene, overcoming these challenges by using only two large centric species from a well-documented sediment core. We will use these records, together with a simple box model, to reconstruct past changes in seawater composition and DSi supply through time.

## 2 Material and methods

Gravity core GeoB3606-1 was collected in the SE Atlantic Ocean (BUS, Fig. 1;  $25^\circ 28' \text{S}$ ,  $13^\circ 05' \text{E}$ ; 1785 m water depth), providing an exceptionally high-resolution paleoclimatic archive of nutrient conditions, productivity, and sea surface temperature (SST) variations off Namibia for the past 70 ka (McKay et al., 2016; Romero et al., 2015, 2003; Romero, 2010; Shukla and Romero, 2018). The robust age model for core GeoB3606-1 has been published elsewhere (Romero, 2010; Romero et al., 2015), with additional radiocarbon dates from McKay et al. (2016). The radiocarbon ages of all samples were converted into calendar years, and a new age model (McKay et al., 2016) was created using the OXCAL 4.2 program with the marine calibration curve MARINE13 (Reimer et al., 2013). High-resolution counts of diatom valves, bulk biogenic components, planktonic and benthic foraminifera stable isotopes, and alkenone-based SSTs have been previously published (Romero, 2010; Romero et al., 2015; McKay et al., 2016). At site GeoB3606-1, diatoms are the main contributors to the opal fraction.

The highest diatom accumulation rate and exceptionally high values of opal (up to 45 wt %), as well as the strongest millennial- and sub-millennial-scale percentage by weight fluctuations, occurred from 70 and 30 ka (Fig. 2). Changes in nutrient supply as a result of enhanced mixing of the uppermost water column, indicated by reduced SSTs as reconstructed from alkenone archives, are unlikely to fully explain variations in diatom productivity alone (Romero et al., 2015). The inverse correlation between the relative abundance of the Antarctic diatom *Fragilariopsis kerguelensis* and the alkenone-based SST variations (Fig. 2) in GeoB3606-1 from 70 to 30 ka suggests a combination of enhanced DSi-rich SO water invasion and stronger wind-driven mixing respectively during this interval of high opal burial (Romero et al., 2003; Shukla and Romero, 2018). In contrast, the warming of the last deglaciation (19–13 ka; Fig. 2) suggests stratification of the uppermost water column, accompanied by a distinctive shift in the diatom assemblage from an upwelling-dominated to a non-upwelling community (Fig. 2), and an increase in calcareous production (Romero et al., 2003).

To better understand these past changes and to deconvolve interactions between DSi supply, utilization in surface waters, and burial in sediments, we constructed a record of  $\delta^{30}\text{Si}$

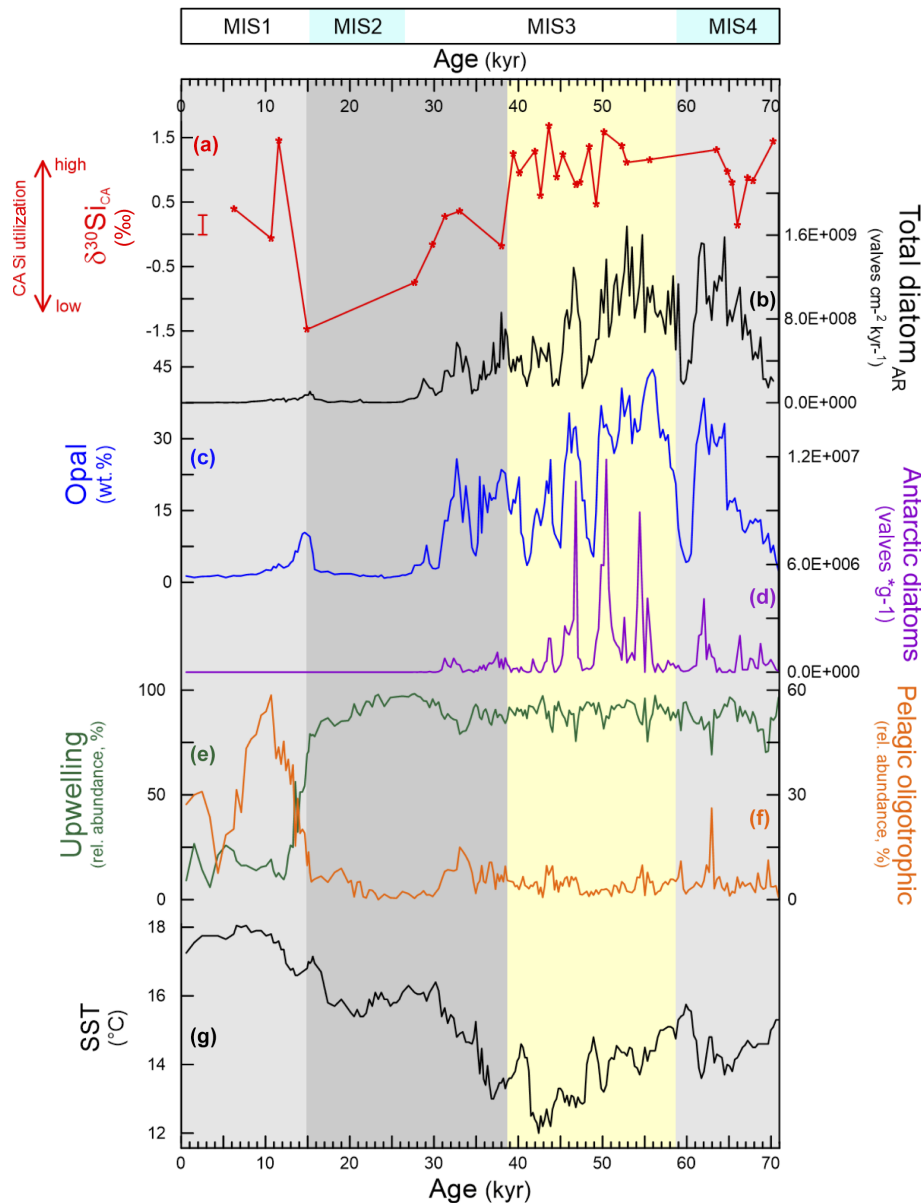


**Figure 2.** Comparison between diatom silicon isotope records and other archives from GeoB3606-1. **(a)**  $\delta^{30}\text{Si}_{\text{CA}}$  records from large diatoms *C. radiatus* and *A. curvatulus* (the error bar shows long-term reproducibility based on repeat measurements of reference standards,  $\pm 2$  SD); **(b)** total diatom accumulation rate; **(c)** opal weight percent; **(d)** abundance of the Antarctic diatom *F. kerguelensis*; **(e)** relative abundance of diatom species characterizing coastal upwelling; **(f)** relative abundance of diatom species characterizing open-ocean or pelagic conditions; **(g)** alkenone-based sea surface temperatures (SSTs; published data from MacKay et al., 2016; Romero, 2010; Romero et al., 2003, 2015). Vertical shaded bars highlight the time periods discussed in Sect. 3.1.

from hand-picked specimens of *Actinocyclus curvatulus* and *Coscinodiscus radiatus* at site GeoB3606-1 (Fig. 2). Single-specimen (or mono-generic)  $\delta^{30}\text{Si}$  diatom archives have previously been constructed to assess Si utilization in particular environments, and they reliably record different absolute values and trends compared to measurements from bulk or other siliceous fractions (Doering et al., 2016a, b; Hendry et al., 2014; Xiong et al., 2015). *A. curvatulus* is a coastal diatom that mainly thrives in shallow, hemipelagic waters bathing

the uppermost slope off Namibia. According to multi-year sediment trap studies off Mauritania, *A. curvatulus* has a higher contribution to the diatom community before and after the main upwelling season (Romero and Fischer, 2017). *C. radiatus* is a common component of planktonic assemblages of tropical and subtropical hemi- to pelagic marine areas (Romero and Fischer, 2017). Compared with *A. curvatulus*, it represents a more “pelagic” signal. However, both species can be considered as occupying niches outside of the



main upwelling zone. Both diatoms are “petri-dish-shaped” and can be considered “large”: diameter up to 200–220  $\mu\text{m}$  (Hasle et al., 1996). Their valves are significantly larger than those of upwelling diatoms (resting spores of *Chaetoceros*, up to 25–30  $\mu\text{m}$  length) and other coastal planktonic taxa (25–50  $\mu\text{m}$ ). This also means that one *A. curvatulus* or *C. radiatus* valve possibly contains 10 to 20 times more opal than the delicate spores of *Chaetoceros* and consume relatively large amounts of DSi in the construction of their valves compared with coastal upwelling diatoms.

As both species grow away from the major upwelling zone, their isotopic compositions (denoted by  $\delta^{30}\text{Si}_{\text{CA}}$  for *Coscinodiscus* and *Actinocyclus*) will reflect a combination of the initial composition of the ambient water and their DSi utilization. Utilization by both species is unlikely to have a quantitative impact on the ambient seawater composition due to the very low overall abundances throughout the record (Romero et al., 2003). Instead, the  $\delta^{30}\text{Si}_{\text{CA}}$  will reflect utilization by the dominant upwelling species (resting spores of *Chaetoceros* spp.).

## 2.1 Laboratory methods

*A. curvatulus* and *C. radiatus* valves were hand-picked from washed and sieved sediments. Valves of the two diatom species were combined to allow for enough material and because the species diatoms are indistinguishable under a low-magnification binocular microscope (note that low MIS2 data resolution was due to limited valve availability). They were the two only large centric diatoms present in the washed and sieved samples of GeoB3606-1. The picked diatoms were transferred to cleaned Teflon vials, and any organic material was removed by drying down in concentrated nitric acid (in-house twice-distilled  $\text{HNO}_3$ ) on a hotplate. The diatoms were dissolved in a strong alkaline solution (0.4 M sodium hydroxide Analar) at 100  $^\circ\text{C}$  overnight. The resulting solution was diluted two-fold in 18 M  $\Omega\text{ cm}$  Milli-Q water and acidified using 6N hydrochloric acid (in-house twice-distilled HCl) to reach a pH of 2–3. The samples were then purified using cation exchange resin (Georg et al., 2006). Analysis of silicon and magnesium isotopes ( $^{28}\text{Si}$ ,  $^{29}\text{Si}$ ,  $^{30}\text{Si}$ ,  $^{24}\text{Mg}$ ,  $^{25}\text{Mg}$ , and  $^{26}\text{Mg}$ ) was carried out in a pilot study by multi-collector inductively coupled plasma mass spectrometry (MC-ICP-MS; Cassarino et al., 2018; Hendry et al., 2015) at the University of Bristol (Thermo Neptune). Further analyses were carried out using similar methodology at the Geochronology and Tracers Facility.

Each sample was filtered, prior to isotopic analysis, to remove any fine particles, which may have eluted off the cation exchange column during the purification stage (Millex-LG, 0.2  $\mu\text{m}$ , PTFE syringe filter, Millipore). Samples and reference materials were acidified using HCl (to a concentration of 0.05 M, using twice quartz-distilled acid) and sulfuric acid ( $\text{H}_2\text{SO}_4$ , to a concentration of 0.003 M, using Romil ultra purity acid). This was done following the recommenda-

tions of Hughes et al. (2011), with the principle being that swamping both samples and reference materials, above and beyond the natural abundance of  $\text{Cl}^-$  and  $\text{SO}_4^{2-}$ , will evoke a similar mass bias response in each. Finally, all samples are doped with 300 ppb magnesium (Mg, Alfa Aesar Spectra-Pure). Spiking with an external element of known isotopic composition allows the data to be monitored and corrected for the effects of instrument-induced mass bias (Cardinal et al., 2003).

In order to resolve isobaric interferences, principally  $^{14}\text{N}^{16}\text{O}^+$  at mass 30, samples were analysed using the medium mass-resolution capability of a Thermo Scientific Neptune Plus MC-ICP-MS, operated in wet-plasma mode. The instrument and sampling details are summarized in Table 1. Using the instrumental parameters outlined, a sensitivity of approximately 4.5 V  $\text{ppm}^{-1}$  was obtained. Data were acquired using a dynamic, two-sequence acquisition (see Tables 1 and 2 for full operating conditions). Faraday amplifier gains were measured at the beginning of each analytical session. Data were collected in one block of 25 ratios, with a resulting analysis time of approximately 12 min per sample (including the sample uptake and stabilization time of 90 s). Blanks were measured on the sample make-up acid (0.05 M HCl, 0.003 M  $\text{H}_2\text{SO}_4$ ) using a shortened version of the acquisition procedure above (one block of 10 ratios). An online background correction was made, with the values obtained for the blank acid subtracted from each succeeding sample. Isotope ratios were calculated using Eqs. (1) and (2).

Reference standards were run to assess the accuracy and precision of the technique (GTF-BGS diatomite  $\delta^{30}\text{Si} + 1.20 \pm 0.16\text{‰}$  (2 SD,  $n = 12$ ); Bristol diatomite  $+1.30 \pm 0.07\text{‰}$  (2 SD internal error,  $n = 1$ ); Bristol LMG08 sponge standard  $-3.43 \pm 0.08\text{‰}$  (2 SD internal error,  $n = 1$ )), which were in good agreement with published values (Reynolds et al., 2007; Hendry et al., 2011). Complete replicate measurements were carried out from three different horizons and reproduced within 0.04 to 0.39  $\text{‰}$ , indicating the natural level of isotopic heterogeneity within a sediment sample. The  $\delta^{29}\text{Si}$  and  $\delta^{30}\text{Si}$  values of standards and samples showed mass-dependent behaviour (slope of three-isotope plot of  $0.50 \pm 0.06$ , consistent with equilibrium or kinetic fractionation; Reynolds et al., 2007). The procedural blank was below the level of detection.

## 2.2 Modelling

A two-box model “thought experiment” was devised in MATLAB to investigate changes in upwelling and biological productivity between simulated MIS3 and late MIS3–MIS2 conditions, based on De La Rocha and Bickle (2005). The model comprised a surface box (area 100 km  $\times$  100 km, with variable depth), and a deep box (area 100 km  $\times$  100 km, water column height 2500 m). There is no evidence for a significant fluvial input along the Namibian coast during the late Quaternary (Shi et al., 2001). As such, relatively low ter-

**Table 1.** Summary of the Neptune Plus MC-ICP-MS operating conditions.

Forward power	1200 W
Reflected power	< 2 W
Plasma gas	16 L min <sup>-1</sup>
Auxiliary gas flow	0.8 L min <sup>-1</sup>
Nebulizer carrier gas flow	1.1 L min <sup>-1</sup>
Nebulizer	ESI PFA-50 (50 $\mu$ L min <sup>-1</sup> uptake rate)
Spray chamber	Thermo Fisher stable sample introduction (SSI) quartz dual cyclonic
Type of detector	Faraday (10 <sup>11</sup> $\Omega$ resistors)
Torch	Demountable glass torch with quartz injector
Cones	Thermo Fisher nickel “H” sample and skimmer
Sample uptake time	90 s
Wash time between samples	10 min

**Table 2.** Summary of the acquisition method used for Si isotope analysis.

	Low four cup	Low three cup	Axial cup	High three cup	High four cup	Integration time (s)	Magnet settle time (s)
Sequence 1		<sup>28</sup> Si	<sup>29</sup> Si	<sup>30</sup> Si		16.8	3
Sequence 1	<sup>24</sup> Mg		<sup>25</sup> Mg		<sup>26</sup> Mg	8.4	3

restrial DSi inputs were set as a constant in the model. The conditions are described in Table 3.

A “MIS3” spin-up is run for 50 000 years to reach steady state, with a deep surface box (100 m). Biological production efficiency (i.e. proportion of available DSi used by diatoms) was set high at 90 %, with strong SO input (approximately 1.5 $\times$  modern) and an export efficiency of 50 % (similar to modern). DSi input is set at 70  $\mu$ M with a  $\delta^{30}\text{DSi}$  of +1.2 ‰, reflecting low utilization in the SO during periods of silicon leakage. Note that although culture studies of *Chaetoceros brevis* revealed a fractionation factor of -2.09 ‰ during growth (Sutton et al., 2013), the fractionation during *Chaetoceros* resting spore formation is unknown; thus, the bulk diatom fractionation is set at -1.1 ‰. Conditions are then changed to simulate the transition into late MIS3–MIS2 (“MIS2”): SO input is dropped to modern concentrations and isotopic composition and biological production efficiency is decreased, and the volume of the surface box is decreased. To test the sensitivity of the system systematically, each of the following parameters was altered one at a time: utilization of diatoms, proportion of SO input, [DSi] (DSi concentration) of SO input, upwelling rate, and volume of the surface box.

### 3 Results and discussion

The downcore  $\delta^{30}\text{Si}_{\text{CA}}$  values range from -1.5 to +1.5 ‰, with the lightest isotopic compositions after 39 ka and the heaviest between 40 and 50 ka as well as after 12 ka (Fig. 2). The model output values after 2000 years are shown in Fig. 3.

These experiments reveal that  $\delta^{30}\text{Si}_{\text{CA}}$  was somewhat sensitive to changes in the SO input of [DSi] and the upwelling rate, with reasonable variation within the model of these parameters allowing for a change in  $\delta^{30}\text{Si}_{\text{CA}}$  of approximately 0.4 ‰ in each case. Changing the surface box volume could achieve a change in  $\delta^{30}\text{Si}_{\text{CA}}$  of approximately 0.8 ‰. Values of  $\delta^{30}\text{Si}_{\text{CA}}$  were most sensitive to utilization (a drop from near-complete utilization to 10 % utilization resulted in a decrease in  $\delta^{30}\text{Si}_{\text{CA}}$  of 1.1 ‰). However, the very isotopically light compositions (where  $\delta^{30}\text{Si}_{\text{CA}} < 0$  ‰) observed in the downcore archive were not achieved by altering only a single parameter at a fixed diatom fractionation factor.

#### 3.1 Diatom utilization intervals in the BUS for the past 70 ka

Using a combination of the new isotopic records as well as published values for opal accumulation and diatom assemblage composition, we can recognize four main intervals within our  $\delta^{30}\text{Si}_{\text{CA}}$  DSi utilization archive (Fig. 4).

##### 3.1.1 Marine Isotope Stage (MIS) 4 (70–60 ka)

During MIS4,  $\delta^{30}\text{Si}_{\text{CA}}$  values are relatively high (approximately +1.5 ‰) but exhibit a pronounced excursion from 70–63 ka towards lighter isotopic compositions, reaching a minimum of approximately 0 ‰ at 66 ka. Cooler SSTs indicate a pulse of upwelling, accompanied by an increase in diatom accumulation, coincident with this excursion. This suggests that there was a transient period of relatively low uti-

**Table 3.** Conditions in the box model.

The surface box is fed from upwelling waters from the deep box. Waters also escape the surface box laterally.
The deep box is fed from incoming waters from the SO and waters escape by upwelling to the surface.
The upwelling rate is set at $4 \times 10^{13} \text{ L yr}^{-1}$ .
Silicon enters the surface box from river run-off (set at an estimated $1 \times 10^6 \text{ mol yr}^{-1}$ ) and from upwelling.
Bulk opal BSi (by dominant upwelling species) is produced in the surface box and results in isotopic fractionation ( $\epsilon = -1.1\text{‰}$ ).
Biological production efficiency (or utilization) and export efficiency are adjustable. Sedimentary preservation is fixed at 3.5 %.
<i>Coscinodiscus</i> and <i>Actinocyclus</i> consume residue (with the same relative utilization as the other diatoms) DSi after bulk opal production, which is assumed to follow an open model for fractionation.

lization by the dominant small-sized *Chaetoceros* spp. as upwelling and export of opal intensified into the early MIS3. In addition to upwelling of marine sources, strong trade winds could have also promoted diatom productivity through the supply of DSi and trace nutrients to surface waters via dust, given the drier conditions on land (Shi et al., 2001; Pichevin et al., 2005).

### 3.1.2 Early MIS3 (60–40 ka)

The early MIS3 is characterized by high but variable  $\delta^{30}\text{Si}_{\text{CA}}$ , ranging between +0.5 and +1.5‰. These high  $\delta^{30}\text{Si}_{\text{CA}}$  values are accompanied by an increase in *F. kerguelensis* and low SST, indicative of strong utilization and a greater input of DSi-rich SO water and intense upwelling.

Strong *Chaetoceros* utilization would have reduced the concentration of preformed DSi exported away from the shelf and uppermost slope waters towards the *A. curvatulus* and *C. radiatus* habitats (hemipelagic and pelagic). *Chaetoceros* production was not only high because of the rate of supply of DSi to coastal waters but also because they were able to use a high proportion of this available DSi. High opal burial is also found during this time interval in sediments from the eastern equatorial Pacific (Kienast et al., 2006), perhaps indicating that this mechanism could have been active in other upwelling zones in the open ocean during MIS3. A similar mechanism may also have been active in the BUS during the Plio-Pleistocene (Etourneau et al., 2012).

The time lag (approximately 10 ka) between the decline in diatom accumulation and  $\delta^{30}\text{Si}_{\text{CA}}$  could be due to a decrease in the DSi concentration of the supplied water after 49 ka (i.e. a decline in SO water, indicated by the decrease in *F. kerguelensis* abundance; Fig. 2). High utilization of waters with a lower DSi concentration would result in lower total opal production and would also potentially contribute towards higher  $\delta^{30}\text{Si}_{\text{CA}}$  values due to prior Si isotopic enrichment of the water. The resolution of  $\delta^{30}\text{Si}_{\text{CA}}$  samples also declines into MIS3 and MIS2, as a result of low diatom abundance, which limits our ability to temporally link the diatom utilization and opal production throughout this period.

### 3.1.3 Late MIS3–MIS2 (40–15 ka)

By the late MIS3, the  $\delta^{30}\text{Si}_{\text{CA}}$  record starts to decline towards lower values, reaching the lowest value of  $-1.5\text{‰}$  by the end of MIS2 (Fig. 2). Weakening upwelling (trends to higher SST) occurred at the same time as the decline towards lower  $\delta^{30}\text{Si}_{\text{CA}}$  values, which points towards a significant decrease in utilization as well as low opal production: as less DSi was being supplied from the SO, diatoms generally declined in abundance. A weak anti-correlation between the size and concentration of *F. kerguelensis* valves at GeoB3606-1 during the late MIS3 (Shukla and Romero, 2018) could indicate an increase in growth rates of these diatoms resulting from a higher Fe availability in the SO due to an enhanced supply of dust (Martínez-García et al., 2014). Alleviation of Fe limitation in the SO could also have caused a decrease in the DSi-to-nitrate uptake ratio of diatoms and, thus, a relative enrichment of DSi in SO waters exported to the lower latitudes (Brzezinski et al., 2002). Although upwelling conditions in surface waters overlying the lower slope off southwestern Africa became less favourable for diatom production, the strength of the trade winds remained strong during MIS2 (Shi et al., 2001), indicating that lower-latitude dust supply is a secondary control on diatom activity in the late Quaternary in the SE Atlantic. The decreased delivery of DSi into the SE Atlantic around 17 ka led to the floral shift at GeoB3606-1 (Fig. 2e). Higher  $\text{CaCO}_3$  (lower opal) values at GeoB3606-1 from late MIS2 to the mid–late Holocene (Romero et al., 2015) indicate a shift in predominant nutrients toward Si-depleted waters. Following the lessened sea ice cover in the SO (Crosta et al., 2005) and the lowered input of Fe south of the polar front due to weakened wind intensity during the last deglaciation (Kohfeld et al., 2005; Sijp and England, 2008), DSi was mainly consumed in waters south of the subantarctic front and became mostly trapped in underlying sediments (Brzezinski et al., 2002; Bradtmiller et al., 2009). This scenario corresponds to the present-day dynamics of production and sedimentation of biogenic particulates in the southern BUS (Romero, 2010), where coccolithophorids dominate primary production over diatoms.

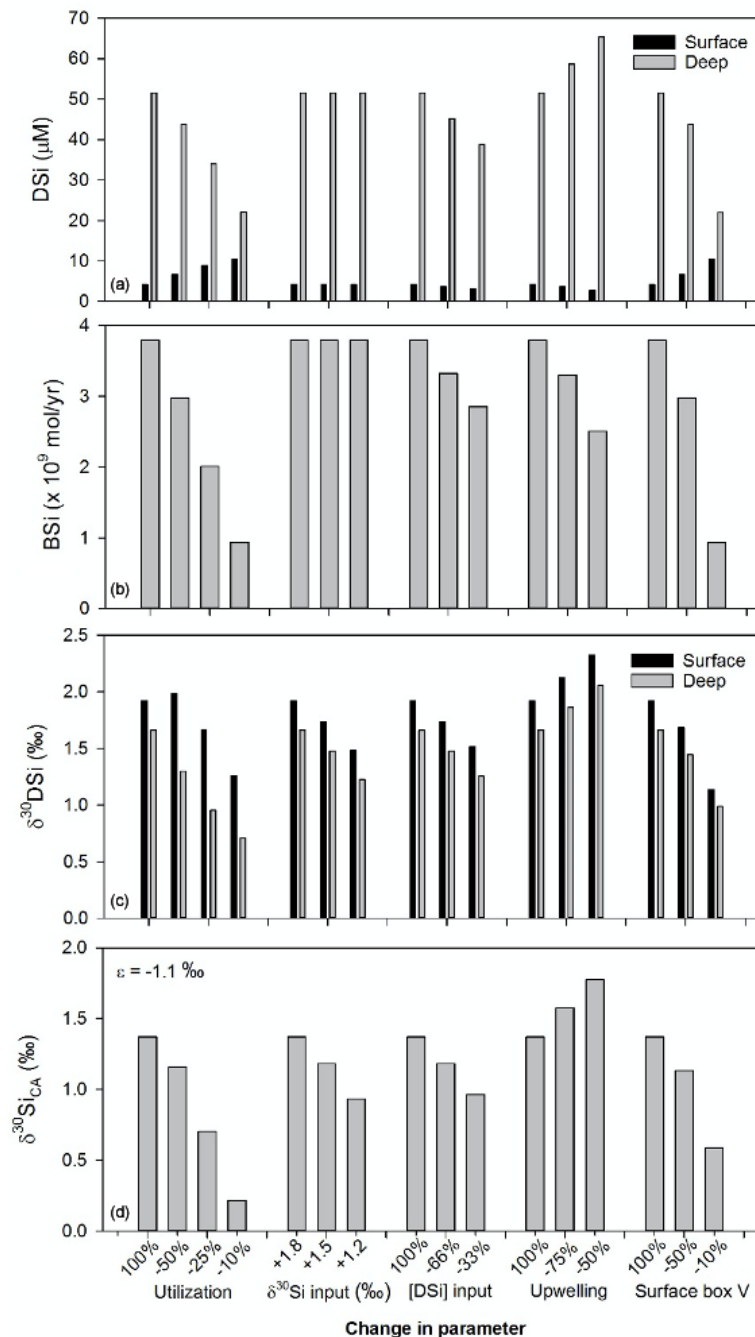


**Figure 3.** Model output results from the two-box model experiments. Each experiment shows the impact on different output parameters from changing one aspect of the model configuration (biological utilization by dominant diatom species, isotopic and [DSi] composition of input waters reflecting a change in SO waters, upwelling strength, and the volume of the surface box): **(a)** seawater [DSi] in the surface and deep box; **(b)** opal production by dominant species; **(c)** the isotopic composition of DSi in the surface and deep box; and **(d)** the isotopic composition of the pelagic diatoms, *C. radiatus* and *A. curvatus* ( $\delta^{30}\text{Si}_{\text{CA}}$ ).

### 3.1.4 MIS1 (15 ka to present)

MIS1 is characterized by a return to higher  $\delta^{30}\text{Si}_{\text{CA}}$  values (approximately 0 to +1.5‰), similar to MIS4 and early MIS3 (Fig. 2a), suggesting a return to high DSi utilization.

The dominance of open-ocean, warm-water diatoms, coupled with low diatom and opal accumulation throughout MIS1, has been interpreted to reflect the predominance of DSi-poor water masses at 25° S in the BUS (Romero, 2010). At the same time as the decline in upwelling intensity (from SST





tion that SO water leaked into the eastern basin of the South Atlantic at this time. If correct, this interpretation would further suggest that this Si-enriched AAIW could have been exported throughout the Atlantic, given that the reconstructed shifts in BUS upwelling and utilization are coincident in time with previous downcore evidence of silica leakage into the western basin during MIS3–MIS4 (Griffiths et al., 2013). However, this silica leakage did not appear to drive strong diatom production throughout the Atlantic and only influenced diatom production in any significant way in the eastern basin, where the thermocline was sufficiently shallow (Abrantes, 2000; Flores et al., 2000; Abrantes, 2003). Despite this, the silica leakage could have driven an increase in diatom production relative to other phytoplankton groups in regions of the eastern Atlantic Basin. The resulting alkalinity shift would have contributed to the drop in atmospheric CO<sub>2</sub> observed in ice cores and the decline into full glacial conditions, thereby supporting the SALH (Matsumoto and Sarmiento, 2008). However, we would suggest that physical oceanographic changes are likely to be largely responsible for the decline in CO<sub>2</sub> during MIS4, which occurred over a much shorter timescale than both the changes in silica cycling within the BUS and the evidence for silica leakage in the eastern basin (Griffiths et al., 2013; Thornalley et al., 2013). Furthermore, the export of Si-enriched SO waters did not last the duration of the last glaciation, and began to decline into late MIS3–MIS2 (i.e. into the LGM), again arguing against a key driving role for biological carbon uptake in controlling atmospheric CO<sub>2</sub>.

### 3.4 Implications for paleonutrients and productivity

The cycling of Si in surface waters and the relationship with organic matter production will be a function of both net production (utilization efficiency and recycling) and export. EBUs are generally characterized by high utilization and export, with rapid turnover. However, the intensity of upwelling and nutrient composition of upwelled waters through time are likely to be sensitive to climate forcings and will impact the balance between utilization and export, the availability of preformed DSi, and the coupling between Si and C cycles (Romero et al., 2003; Romero, 2010; Hendry and Brzezinski, 2014). Using a combination of  $\delta^{30}\text{Si}$ , diatom assemblages, opal accumulation, and alkenone-based SSTs allows the investigation of how the diatom community was using supplied DSi in the surface waters during periods of rapid climate variations in low-latitude EBUs. We have shown that this approach can be successfully used in the BUS to produce a continuous record across full glacial conditions to investigate the impact of SO leakage and ventilation on diatom production in surface waters. This approach is a promising means to assess the impact of water mass variations on Si cycling by diatoms in other environmental settings, where downcore diatom assemblages have already been recorded. Upwelling areas (e.g. equatorial regions and frontal zones) are ideal tar-

gets, given their sensitivity to rapid changes in ocean mixing and subsurface nutrient supply. By carefully selecting identifiable and well-constrained diatom species for isotopic analysis, DSi utilization and production can be quantified more robustly, without uncertainties arising from seasonality or ecological niche conditions.

**Data availability.** All data are available for download at <https://doi.pangaea.de/10.1594/PANGAEA.921237> (Hendry et al., 2020).

**Author contributions.** OR and KH devised the study, and KH and VP carried out the isotope analyses. All authors were involved in the preparation of the paper.

**Competing interests.** The authors declare that they have no conflict of interest.

**Acknowledgements.** The authors would like to thank Stephanie Bates for help in the laboratory and Gregory de Souza for advice on box modelling. Lisa Mehring is acknowledged for her work in preparing samples for Si measurements.

**Financial support.** This research has been supported by the Royal Society (grant no. URF/R/180021 and RG130386) and the Deutsche Forschungsgemeinschaft (grant no. RO3039/9-1).

**Review statement.** This paper was edited by Erin McClymont and reviewed by two anonymous referees.

### References

- Abrantes, F.: 200 000 yr diatom records from Atlantic upwelling sites reveal maximum productivity during LGM and a shift in phytoplankton community structure at 185 000 yr, *Earth Planet. Sci. Lett.*, 176, 7–16, 2000.
- Abrantes, F.: A 340,000 year continental climate record from tropical Africa – news from opal phytoliths from the equatorial Atlantic, *Earth Planet. Sci. Lett.*, 209, 165–179, 2003.
- Berger, W. and Wefer, G.: Expeditions into the past: paleoceanographic studies in the South Atlantic, in: *The South Atlantic*, edited by: Wefer, G., Berger, W. H., Siedler, G., and Webb, D. J., Springer, Berlin, Heidelberg, Germany, 363–410, 1996.
- Berger, W. H., Lange, C. B., and Wefer, G.: Upwelling history of the Benguela-Namibia system: A synthesis of Leg 175 results, *Proceedings of the Ocean Drilling Program, Scientific Results*, 175, 1–103, 2002.
- Bradt Miller, L., Anderson, R., Fleisher, M., and Burckle, L.: Diatom productivity in the equatorial Pacific Ocean from the last glacial period to the present: A test of the silicic acid leakage hypothesis, *Paleoceanography*, 21, PA4201, <https://doi.org/10.1029/2006PA001282>, 2006.

- Bradt Miller, L., Anderson, R., Fleisher, M., and Burckle, L.: Opal burial in the equatorial Atlantic Ocean over the last 30 kyr: Implications for glacial-interglacial silica distribution, *Paleoceanography*, 22, PA4216, <https://doi.org/10.1029/2007PA001443>, 2007.
- Bradt Miller, L., Anderson, R., Fleisher, M., and Burckle, L.: Comparing glacial and Holocene opal fluxes in the Pacific sector of the Southern Ocean, *Paleoceanography* 24, PA2214, <https://doi.org/10.1029/2008PA001693>, 2009.
- Brzezinski, M. A., Pride, C. J., Franck, V. M., Sigman, D. M., Sarmiento, J. L., Matsumoto, K., Gruber, N., Rau, G. H., and Coale, K. H.: A switch from  $\text{Si}(\text{OH})_4$  to  $\text{NO}_3^-$  depletion in the glacial Southern Ocean, *Geophys. Res. Lett.*, 29, 1564, <https://doi.org/10.1029/2001GL014349>, 2002.
- Cardinal, D., Alleman, L. Y., de Jong, J., Ziegler, K., and André, L.: Isotopic composition of silicon measured by multicollector plasma source mass spectrometry in dry plasma mode, *J. Anal. Atom. Spectrom.*, 18, 213–218, 2003.
- Cassarino, L., Coath, C. D., Xavier, J. R., and Hendry, K. R.: Silicon isotopes of deep sea sponges: new insights into biomineralisation and skeletal structure, *Biogeosciences*, 15, 6959–6977, <https://doi.org/10.5194/bg-15-6959-2018>, 2018.
- Chase, Z., Anderson, R. F., Fleisher, M. Q., and Kubik, P. W.: Accumulation of biogenic and lithogenic material in the Pacific sector of the Southern Ocean during the past 40,000 years, *Deep Sea Res.*, 50, 799–832, 2003.
- Crosta, X., Shemesh, A., Etourneau, J., Yam, R., Billy, I., and Pichon, J.: Nutrient cycling in the Indian sector of the Southern Ocean over the last 50,000 years, *Global Biogeochem. Cy.*, 19, GB3007, <https://doi.org/10.1029/2004GB002344>, 2005.
- De La Rocha, C. and Bickle, M. J.: Sensitivity of silicon isotopes to whole-ocean changes in the silica cycle, *Mar. Geol.*, 217, 267–282, 2005.
- De La Rocha, C. L., Brzezinski, M. A., and DeNiro, M. J.: Fractionation of silicon isotopes by marine diatoms during biogenic silica formation, *Geochim. Cosmochim. Ac.*, 61, 5051–5056, 1997.
- Doering, K., Ehlert, C., Grasse, P., Crosta, X., Fleury, S., Frank, M., and Schneider, R.: Differences between mono-generic and mixed diatom silicon isotope compositions trace present and past nutrient utilisation off Peru, *Geochim. Cosmochim. Ac.*, 177, 30–47, 2016a.
- Doering, K., Erdem, Z., Ehlert, C., Fleury, S., Frank, M., and Schneider, R.: Changes in diatom productivity and upwelling intensity off Peru since the Last Glacial Maximum: Response to basin-scale atmospheric and oceanic forcing, *Paleoceanography*, 31, 1453–1473, 2016b.
- Dubois, N., Kienast, M., Kienast, S., Calvert, S. E., François, R., and Anderson, R. F.: Sedimentary opal records in the eastern equatorial Pacific: It is not all about leakage, *Global Biogeochem. Cy.*, 24, GB4020, <https://doi.org/10.1029/2010GB003821>, 2010.
- Etourneau, J., Ehlert, C., Frank, M., Martinez, P., and Schneider, R.: Contribution of changes in opal productivity and nutrient distribution in the coastal upwelling systems to Late Pliocene/Early Pleistocene climate cooling, *Clim. Past*, 8, 1435–1445, <https://doi.org/10.5194/cp-8-1435-2012>, 2012.
- Flores, J.-A., Bárcena, M., and Sierro, F.: Ocean-surface and wind dynamics in the Atlantic Ocean off Northwest Africa during the last 140 000 years, *Palaeogeogr. Palaeoclimatol.*, 161, 459–478, 2000.
- Georg, R. B., Reynolds, B. C., Frank, M., and Halliday, A. N.: New sample preparation techniques for the determination of Si isotopic compositions using MC-ICPMS, *Chem. Geol.*, 235, 95–104, <https://doi.org/10.1016/j.chemgeo.2006.06.006>, 2006.
- Griffiths, J. D., Barker, S., Hendry, K. R., Thornalley, D. J., van de Flierdt, T., Hall, I. R., and Anderson, R. F.: Evidence of silicic acid leakage to the tropical Atlantic via Antarctic Intermediate Water during Marine Isotope Stage 4, *Paleoceanography*, 28, 307–318, 2013.
- Hasle, G. R., Syvertsen, E. E., Steidinger, K. A., Tangen, K., and Tomas, C. R.: Identifying marine diatoms and dinoflagellates, Elsevier Academic Press, San Diego, USA, 1996.
- Hendry, K. R. and Brzezinski, M. A.: Using silicon isotopes to understand the role of the Southern Ocean in modern and ancient biogeochemistry and climate, *Quatern. Sci. Rev.*, 89, 13–26, 2014.
- Hendry, K. R., Leng, M. J., Robinson, L. F., Sloane, H. J., Blusztjan, J., Rickaby, R. E., Georg, R. B., and Halliday, A. N.: Silicon isotopes in Antarctic sponges: an interlaboratory comparison, *Antarctic Sci.*, 23, 34–42, 2011.
- Hendry, K. R., Robinson, L. F., McManus, J. F., and Hays, J. D.: Silicon isotopes indicate enhanced carbon export efficiency in the North Atlantic during deglaciation, *Nat. Commun.*, 5, 1–9, 2014.
- Hendry, K. R., Swann, G. E. A., Leng, M. J., Sloane, H. J., Goodwin, C., Berman, J., and Maldonado, M.: Technical Note: Silica stable isotopes and silicification in a carnivorous sponge *Asbestopluma* sp., *Biogeosciences*, 12, 3489–3498, <https://doi.org/10.5194/bg-12-3489-2015>, 2015.
- Hendry, K. R., Gong, X., Knorr, G., Pike, J., and Hall, I. R.: Deglacial diatom production in the tropical North Atlantic driven by enhanced silicic acid supply, *Earth Planet. Sci. Lett.*, 438, 122–129, 2016.
- Hendry, K. R., Romero, O. E., and Pashley, V.:  $\delta^{30}\text{Si}$  data measured on two diatom species in sediment core GeoB3606-1, PAN-GAEA, <https://doi.org/10.1594/PANGAEA.921237>, 2020.
- Horn, M. G., Beucher, C. P., Robinson, R. S., and Brzezinski, M. A.: Southern ocean nitrogen and silicon dynamics during the last deglaciation, *Earth Planet. Sci. Lett.*, 310, 334–339, 2011.
- Kienast, S., Kienast, M., Jaccard, S., Calvert, S., and François, R.: Testing the silica leakage hypothesis with sedimentary opal records from the eastern equatorial Pacific over the last 150 kyrs, *Geophys. Res. Lett.*, 33, L15607, <https://doi.org/10.1029/2006GL026651>, 2006.
- Kohfeld, K. E., Le Quéré, C., Harrison, S. P., and Anderson, R. F.: Role of marine biology in glacial-interglacial  $\text{CO}_2$  cycles, *Science*, 308, 74–78, 2005.
- Martínez-García, A., Sigman, D. M., Ren, H., Anderson, R. F., Straub, M., Hodell, D. A., Jaccard, S. L., Eglinton, T. I., and Haug, G. H.: Iron fertilization of the Subantarctic Ocean during the last ice age, *Science*, 343, 1347–1350, 2014.
- Matsumoto, K. and Sarmiento, J.: A corollary to the silicic acid leakage hypothesis, *Paleoceanography* 23, PA2203, <https://doi.org/10.1029/2007PA001515>, 2008.
- McKay, C., Filipsson, H. L., Romero, O. E., Stuut, J.-B., and Björck, S.: The interplay between the surface and bottom water environment within the Benguela Upwelling System over the last 70 ka, *Paleoceanography*, 31, 266–285, 2016.

- Meckler, A. N., Sigman, D. M., Gibson, K. A., François, R., Martinez-Garcia, A., Jaccard, S. L., Röhl, U., Peterson, L. C., Tiedemann, R., and Haug, G. H.: Deglacial pulses of deep-ocean silicate into the subtropical North Atlantic Ocean, *Nature*, 495, 495–498, 2013.
- Pichevin, L., Cremer, M., Giraudeau, J., and Bertrand, P.: A 190 ky record of lithogenic grain-size on the Namibian slope: Forging a tight link between past wind-strength and coastal upwelling dynamics, *Mar. Geol.*, 218, 81–96, 2005.
- Ragueneau, O., Tréguer, P., Leynaert, A., Anderson, R. F., Brzezinski, M. A., DeMaster, D. J., Dugdale, R. C., Dymond, J., Fischer, G., François, R., Heinze, C., Maier-Reimer, E., Martin-Jézéquel, V., Nelson, D. M., and Quéguiner, B.: A review of the Si cycle in the modern ocean: recent progress and missing gaps in the application of biogenic opal as a paleoproductivity proxy, *Global Planet. Change*, 26, 317–365, 2000.
- Reimer, P. J., Bard, E., Bayliss, A., Beck, J. W., Blackwell, P. G., Ramsey, C. B., Buck, C. E., Cheng, H., Edwards, R. L., Friedrich, M., Grootes, P. M., Guilderson, T. P., Hafliðason, H., Hajdas, I., Hatté, C., Heaton, T. J., Hoffmann, D. L., Hogg, A. G., Hughen, K. A., Kaiser, K. F., Kromer, B., Manning, S. W., Niu, M., Reimer, Ron W., Richards, D. A., Scott, E. M., Southon, J. R., Staff, R. A., Turney, C. S. M., and van der Plicht, J.: IntCal13 and Marine13 radiocarbon age calibration curves 0–50,000 years cal BP, *Radiocarbon*, 55, 1869–1887, 2013.
- Reynolds, B. C., Aggarwal, J., Andre, L., Baxter, D., Beucher, C., Brzezinski, M. A., Engstrom, E., Georg, R. B., Land, M., Leng, M. J., Opfergelt, S., Rodushkin, I., Sloane, H. J., van den Boorn, S. H. J. M., Vroon, P. Z., and Cardinal, D.: An inter-laboratory comparison of Si isotope reference materials, *J. Anal. Atom. Spectron.*, 22, 561–568, <https://doi.org/10.1039/b616755a>, 2007.
- Romero, O.: Changes in style and intensity of production in the Southeastern Atlantic over the last 70,000 yr, *Mar. Micropaleontol.*, 74, 15–28, 2010.
- Romero, O., Mollenhauer, G., Schneider, R. R., and Wefer, G.: Oscillations of the siliceous imprint in the central Benguela Upwelling System from MIS 3 through to the early Holocene: the influence of the Southern Ocean, *J. Quatern. Sci.*, 18, 733–743, 2003.
- Romero, O., Crosta, X., Kim, J.-H., Pichevin, L., and Crespin, J.: Rapid longitudinal migrations of the filament front off Namibia (SE Atlantic) during the past 70 kyr, *Global Planet. Change*, 125, 1–12, 2015.
- Romero, O. E. and Fischer, G.: Shift in the species composition of the diatom community in the eutrophic Mauritanian coastal upwelling: Results from a multi-year sediment trap experiment (2003–2010), *Prog. Oceanogr.*, 159, 31–44, 2017.
- Rousseau, J., Ellwood, M. J., Bostock, H., and Neil, H.: Estimates of late Quaternary mode and intermediate water silicic acid concentration in the Pacific Southern Ocean, *Earth Planet. Sci. Lett.*, 439, 101–108, 2016.
- Shi, N., Schneider, R., Beug, H.-J., and Dupont, L. M.: Southeast trade wind variations during the last 135 kyr: evidence from pollen spectra in eastern South Atlantic sediments, *Earth Planet. Sci. Lett.*, 187, 311–321, 2001.
- Shukla, S. K. and Romero, O. E.: Glacial valve size variation of the Southern Ocean diatom *Fragilariopsis kerguelensis* preserved in the Benguela Upwelling System, southeastern Atlantic, *Palaeogeogr. Palaeoclimatol.*, 499, 112–122, 2018.
- Sijp, W. P. and England, M. H.: The effect of a northward shift in the southern hemisphere westerlies on the global ocean, *Prog. Oceanogr.*, 79, 1–19, 2008.
- Sutton, J. N., Varela, D. E., Brzezinski, M. A., and Beucher, C. P.: Species-dependent silicon isotope fractionation by marine diatoms, *Geochim. Cosmochim. Ac.*, 104, 300–309, 2013.
- Swann, G. E., Pike, J., Leng, M. J., Sloane, H. J., and Snelling, A. M.: Temporal controls on silicic acid utilisation along the West Antarctic Peninsula, *Nat. Commun.*, 8, 1–8, 2017.
- Thornalley, D. J., Barker, S., Becker, J., Hall, I. R., and Knorr, G.: Abrupt changes in deep Atlantic circulation during the transition to full glacial conditions, *Paleoceanography*, 28, 253–262, 2013.
- Tréguer, P., Bowler, C., Moriceau, B., Dutkiewicz, S., Gehlen, M., Aumont, P., Bittner, L., Dugdale, R., Finkel, Z., Iudicone, D., Jahn, O., Guidi, L., Lasbleiz, M., Leblanc, K., Levy, M., and Pondaven, P.: Influence of diatom diversity on the ocean biological carbon pump, *Nat. Geosci.*, 11, 27–37, 2018.
- Xiong, Z., Li, T., Algeo, T., Doering, K., Frank, M., Brzezinski, M. A., Chang, F., Opfergelt, S., Crosta, X., Jiang, F., Wan, S. and Zhai, B.: The silicon isotope composition of *Ethmodiscus rex* laminated diatom mats from the tropical West Pacific: Implications for silicate cycling during the Last Glacial Maximum, *Paleoceanography*, 30, 803–823, 2015.